

Inversion in a four-terminal superconducting device on the quartet line: I. Two-dimensional metal and the quartet beam splitter

Régis Mélin¹

¹Univ. Grenoble-Alpes, CNRS, Grenoble INP, Institut NEEL, 38000 Grenoble, France

In connection with the recent Harvard group experiment on the quartets in a graphene-based four-terminal Josephson junction containing a loop, we establish the predictions of lowest-order perturbation theory in the tunnel amplitudes between a two-dimensional (2D) metal and four superconducting leads. The critical current on the quartet line $I_c(\Phi/\Phi_0)$ depends on the reduced flux Φ/Φ_0 and it results from an interference between the three-terminal quartets and a nonstandard four-terminal process of split quartets (SQ). The SQ result from synchronizing two Josephson junctions by the 2D quantum nanowake effect, already in the adiabatic limit. We establish that the SQ are π -shifted in perturbation theory, because they involve quantum mechanical exchange of a quasiparticle among two Cooper pairs. It is shown for arbitrary interface transparencies and bias voltage that “Observation of $I_c(0) \neq I_c(1/2)$ ” implies “Evidence for the SQ”. It is concluded that the recent experiment mentioned above finds evidence for the SQ.

I. INTRODUCTION

A superconductor such as Aluminum is characterized by a macroscopic phase variable φ and a gap Δ separating the collective BCS ground state from the first quasiparticles. A BCS superconductor supports a dissipationless supercurrent flow, in response to phase gradients.

BCS theory assigns given numerical values to the phase φ of a single superconductor, even if φ is a nongauge-invariant quantity which cannot be observed under any experimental condition. BCS theory also yields absence of the Meissner effect, *i.e.* a magnetic field is not repelled by a BCS superconductor. These paradoxes were resolved^{1,2} by the so-called Higgs mechanism *i.e.* a theory of superconductivity which takes Coulomb interactions into account, and describes the dynamics of the collective modes in the so-called “mexican-hat” potential.

Following the seminal works^{1,2} on gauge invariance mentioned above, Josephson calculated³ the supercurrent flowing through a tunnel junction connecting two superconductors S_1 and S_2 with phases φ_1 and φ_2 . The phase φ of a single superconductor is not gauge invariant, thus it is not observable. The difference $\varphi_1 - \varphi_2$ between the phases of S_1 and S_2 is gauge-invariant. The latter is observable as the following dissipationless current through a superconductor-insulator-superconductor S_1IS_2 Josephson junction:

$$I = I_c^{(2T)} \sin(\varphi_1 - \varphi_2), \quad (1)$$

which has maximal value set by the critical current $I_c^{(2T)}$.

Eq. (1) describes the tunneling of a single Cooper pair between S_1 and S_2 . Composite objects made of two or more Cooper pairs can tunnel in the same quantum event for larger values of the contact transparencies. The possibility of two-Cooper pair tunneling yields the $\sin(2(\varphi_1 - \varphi_2))$ term in the following equation:

$$I = \left[I_c^{(1),1} + I_c^{(2),1} + \dots \right] \sin(\varphi_1 - \varphi_2) \quad (2)$$

$$+ \left[I_c^{(2),2} + \dots \right] \sin(2(\varphi_1 - \varphi_2)) \quad (3)$$

$$+ \dots \quad (4)$$

Due to their internal structure, the two Cooper pairs are coupled to each other by the Fermi exclusion principle since they are located within the same coherence volume $\sim \xi^3$ in the same time window $\tau_\Delta = \hbar/\Delta$, where the zero-energy coherence length ξ is given by $\xi = \hbar v_F/\Delta$, with v_F the Fermi velocity.

The expansion given by Eqs. (2)-(4) shows fast convergence under usual experimental conditions: Eqs. (2)-(4) are usually dominated by $I_c^{(1),1}$, such that $|I_c^{(1),1}| \gg |I_c^{(2),1}|$ and $|I_c^{(1),1}| \gg |I_c^{(2),2}|$.

The following article deals with describing how two Cooper pairs couple to each other in the multiterminal Josephson effect, in connection with interpretation of a recent experiment realized in the Harvard group⁴.

Higher-order harmonics of the Josephson relation can indeed be accessed experimentally in *multiterminal Josephson junctions*, where the term similar to $I_c^{(1),1} + I_c^{(2),1} + \dots$ in Eq. (2) can be made ac, typically in the range of a GHz or 10 GHz. This offers experimental signal dominated by a higher-order dc-contribution similar to $I_c^{(2),2} + \dots$ in Eq. (3).

Concerning multiterminal Josephson junctions, it was shown⁵⁻¹² that nonstandard effects appear in “supercurrent splitting”, if three superconducting leads are connected at distance shorter than $\sim \xi$. This four-fermion quartet resonance can be viewed as being “glued” by the interfaces, in absence of pre-existing quartets in the bulk of the BCS superconductors. The quartets are revealed under voltage biasing (S_a, S_b, S_c) at (V_a, V_b, V_c). Namely, energy conservation puts a constraint on the voltages V_a and V_b which have to be located on the “quartet line” $V_a + V_b = 0$ in the (V_a, V_b) voltage plane (S_c being grounded at $V_c = 0$). The predicted⁵⁻¹² Josephson anomaly on the quartet line $V_a + V_b = 0$ originates from synchronizing the three superconductors (S_a, S_b, S_c), *via* the following gauge-invariant static combination of their respective macroscopic phase variables:

$$\varphi_q = \varphi_a + \varphi_b - 2\varphi_c. \quad (5)$$

The Josephson relations imply that the phase combination $\varphi_a(t) + \varphi_b(t) - 2\varphi_c(t)$ is time t -independent, with $\varphi_a(t) = 2eVt/\hbar + \varphi_a$, $\varphi_b(t) = -2eVt/\hbar + \varphi_b$, and $\varphi_c(t) = \varphi_c$. The

previous difference $\varphi_1 - \varphi_2$ between the phases φ_1 and φ_2 of S_1 and S_2 enters the two-terminal dc-Josephson current-phase relation given by Eq. (1). Conversely, in a three-terminal Josephson junction, the nonstandard combination given by Eq. (5) implies that the quartet current I_q is given by

$$I_q = I_{c,q} \sin \varphi_q \quad (6)$$

in the limit of tunnel contacts. Eq. (6) depends on the phases of the three superconductors through the quartet phase φ_q in Eq. (5), not only on the difference $\varphi_1 - \varphi_2$ such as in Eq. (1) for the two-terminal dc-Josephson effect.

The prediction of the quartets was confirmed experimentally by the Grenoble group¹³ (with a metallic structure) and the Weizmann Institute group¹⁴ (with a semiconducting nanowire double quantum dot). The recent Harvard group experiment⁴ provides evidence for unanticipated features of the quartets in the graphene-based four-terminal device shown on figure 1, in connection with the additional parameter provided by the flux Φ through the loop.

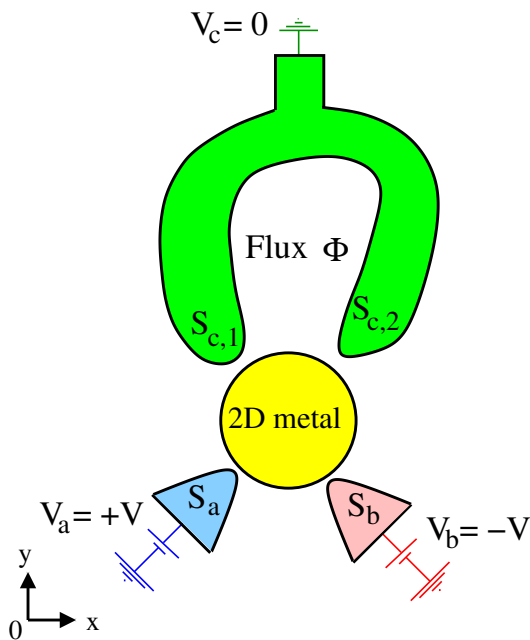


FIG. 1. *The four-terminal superconducting device.* The superconducting leads S_a , S_b and S_c are voltage-biased at $(V_a, V_b, 0)$, with $V_a = -V_b \equiv V$ on the quartet line. The loop defined in the grounded S_c has contact points $S_{c,1}$ and $S_{c,2}$ on the 2D metal which is realized with graphene gated away from the Dirac points in the Harvard group experiment⁴. A flux Φ is piercing through the loop.

The four-terminal Josephson junction in figure 1 is an opportunity for investigating interference in the quartet current, in the spirit of a superconducting quantum interference device (SQUID)¹⁵. Several experiments on multiterminal devices containing loops have been proposed recently^{7,16,17} in absence of voltage biasing, *i.e.* at equilibrium, where all parts of the circuit are grounded. For instance, the device shown in figure 1 was proposed recently^{18,19} in the perspective of producing Weyl points and nontrivial topology in a

four-terminal Josephson junction. The voltage biasing conditions are different in Refs. 18 and 19 for topology and in our work for the quartets: in Refs. 18 and 19, the voltages are such as to integrate the Berry curvature in the transconductance *i.e.* they are incommensurate, so as to sweep the (φ_a, φ_b) Brillouin zone of the superconducting phases. Experiments related to the theoretical proposal on topology^{18,19} were attempted^{20–22}. Coming back to the quartets in the Harvard group experiment⁴, the $(S_a, S_b, S_{c,1}, S_{c,2})$ four-terminal device is biased at (V_a, V_b, V_c, V_c) , where $V_c = 0$ is the reference voltage of the grounded loop S_c terminated by $S_{c,1}$ and $S_{c,2}$ (see figure 1). In this sequence of papers I, II and III, we consider biasing on the quartet line $V_a + V_b = 0$, *i.e.* $V_a = V$ and $V_b = -V$. Our strategy is to develop a theory which is intended to interpret the following unexpected features reported by the Harvard group⁴:

(i) A quartet Josephson anomaly appears on the $V_a + V_b = 0$ quartet line, once one of the elements of the conductance matrix is plotted as a colorplot in the (V_a, V_b) voltage plane. This is compatible with the theoretical prediction of the quartets for three superconducting terminals^{5–12}, and with the previous Grenoble¹³ and Weizmann Institute¹⁴ group experiments.

(ii) In addition, in the Harvard group experiment⁴, the quartet current in the four terminal configuration of figure 1 is modulated with the reduced flux Φ/Φ_0 piercing through the loop.

(iii) An “inversion” appears experimentally in a given voltage window, once the quartet signal is plotted as a function of Φ/Φ_0 . Namely, the quartet anomaly can be stronger at $\Phi/\Phi_0 = 1/2$ than at $\Phi/\Phi_0 = 0$. On the contrary, superconductivity is naively expected to be stronger at $\Phi/\Phi_0 = 0$ than at $\Phi/\Phi_0 = 1/2$, due to destructive interferences. “Non inverted behavior” is also obtained in other voltage windows. The following paper I addresses a theoretical description of this “non inverted behavior” on the basis of the simplest $V = 0^+$ adiabatic limit. The next paper II addresses the theory of an inversion controlled by the bias voltage V on the quartet line.

(iv) A small voltage scale $V_* \ll \Delta$ emerges in the voltage V -dependence of the quartet signal. The last paper III of the series addresses emergence of a small energy scale.

In the following paper I, we propose a simple model for the Harvard group experiment⁴ (see sections IV, V and VI), and next, the model is analyzed in connection with the experiment (see sections VII, VIII and IX).

The detailed structure of the paper is the following. Section II summarizes the three papers of the series. The Hamiltonians are given in section III. The quartets and the SQ are presented in section IV, as well as the resulting current-phase relations. Section V deals with the interference in the critical current between the quartets and the SQ. The importance of two space dimensions (see the yellow intermediate region in figure 1) is discussed in section VI. Section VII demonstrates that π -shifts are obtained from perturbation theory in the quartet and the SQ channels. Section VIII shows that this implies absence of inversion in the critical current I_c between the reduced flux values $\Phi/\Phi_0 = 0$ and $\Phi/\Phi_0 = 1/2$. Section VIII also addresses the information to be deduced from the comparison between the values of the critical current at reduced

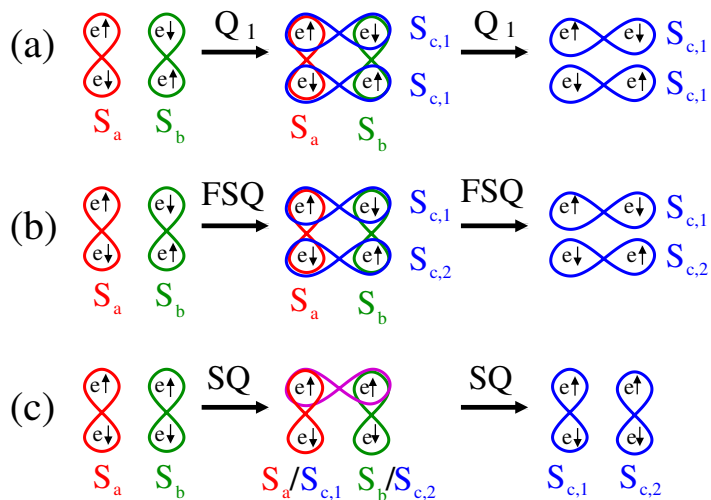


FIG. 2. Artist view of the microscopic processes consisting of: the Q_1 -quartets (panel a), the statistical fluctuations of the split quartet current (FSQ, panel b) and the split quartets (SQ, panel c). Two pairs are taken from S_a and S_b biased at $\pm V$. They exchange partners according to the “intermediate state” represented schematically. The outgoing state is produced, with two pairs transmitted into $S_{c,1}$ (Q_1 -quartets on panel a), or one pair transmitted into $S_{c,1}$ and another one into $S_{c,2}$ (FSQ on panel b and SQ on panel c). A four-particle resonance is produced for the quartets and the FSQ on panels a and b, *i.e.* the two Cooper pairs from S_a and S_b recombine after exchanging partners. The SQ on panel c involve interchanging a quasiparticle between the two Cooper pairs from S_a and S_b . Thus, the microscopic mechanism is different for the quartets and the FSQ (panels a and b), or for the SQ (panel c).

fluxes $\Phi/\Phi_0 = 0$ and $\Phi/\Phi_0 = 1/2$. Section IX presents exact results for arbitrary contact transparencies and voltage. A summary and final remarks are given in section X.

II. THE THREE PAPERS OF THE SERIES

In this section, we provide a presentation of the three papers of the series. The following items (A), (B) and (C) detail which features of the Harvard group experiment⁴ will be addressed and explained in the different papers I, II and III:

(A) The following “paper I” provides the simplest predictive approach, *i.e.* perturbation theory in the contact transparencies in the adiabatic limit where $(S_a, S_b, S_{c,1}, S_{c,2})$ are biased at $(V, -V, 0, 0)$ on the quartet line, with $V = 0^+$. In the context of Cooper pair splitting in a three-terminal normal metal-superconductor-normal metal (NSN) device, a similar perturbative approach²³ turned out to usefully uncover the important elementary processes of “Elastic Cotunneling” and “Crossed Andreev reflection”. Concerning the four-terminal Josephson junction on figure 1, the perturbative calculations presented below provide evidence for the expected “Three-terminal quartets”, interfering with the nonstandard channel of the “Split Quartets”.

More precisely, lowest order perturbation theory predicts three processes which are shown as an artist view in figures 2a, b and c:

(a) *The quartets* in which two pairs (from S_a and from S_b biased at $\pm V$ respectively) exchange partners and recombine as two outgoing pairs transmitted at the same contact $S_{c,1}$ (or at the contact $S_{c,2}$).

(b) *The statistical fluctuations of the split quartets* (FSQ) take one pair from S_a , another one from S_b biased at $\pm V$ respectively, split and recombine them as outgoing pairs, one of those being transmitted into $S_{c,1}$, and the other one being transmitted into $S_{c,2}$. The FSQ solely contribute to sample-to-sample statistical fluctuations of the supercurrent.

(c) *The split quartets* (SQ) interchange a quasiparticle between two pairs taken from S_a and S_b biased at $\pm V$ respectively. An outgoing pair is transmitted into $S_{c,1}$ and another

one into $S_{c,2}$. The SQ realize a “four-terminal quartet beam splitter”, namely, they take two pairs from S_a and S_b , make their wave-function overlap and transmit a pair into $S_{c,1}$ and another one into $S_{c,2}$ in the outgoing state.

The quartets (item a above) and the SQ (item c above) are π -shifted, due to the “minus” sign in the wave-function of a Cooper pair for the former, and to interchanging two quasiparticles for the latter. The critical current at $\Phi/\Phi_0 = 0$ is larger than at $\Phi/\Phi_0 = 1/2$.

At first glance, the absence of inversion between $\Phi/\Phi_0 = 0$ and $\Phi/\Phi_0 = 1/2$ may be considered as being “conventional” and thus less spectacular than “inverted behavior”. However, it turns out that this noninverted behavior originates from an interference between the quartets and the SQ, which have both a highly nontrivial π -shift of quantum mechanical origin.

Now, we provide items (B) and (C) summarizing the goals of papers II and III of this series, in connection with explaining the Harvard group experiment⁴:

(B) While the following paper I is based essentially on low-transparency interfaces and on the $V = 0^+$ adiabatic limit, we propose in the next paper II a generic Floquet mechanism by which an inversion between $\Phi/\Phi_0 = 0$ and $\Phi/\Phi_0 = 1/2$ can be produced by tuning the bias voltage V on the quartet line. Most of the description in this paper II is based on a simplifying zero-dimensional quantum dot configuration supporting a single level at zero energy. A link is established, which relates the inversion between $\Phi/\Phi_0 = 0$ and $\Phi/\Phi_0 = 1/2$ in the critical current to repulsion between the Floquet levels as a function of bias voltage V on the quartet line. In this paper II, robustness of the inversion is also established with respect to crossing-over from weak to strong Landau-Zener tunneling upon varying the couplings between the dot and the superconducting leads, and with respect to introducing several energy levels in a multilevel quantum dot.

(C) The last paper III of the series establishes a link to the physics of the proximity effect, however taking the specificities of the quartets and the SQ through a 2D metal into account. In order to illustrate this point, let us consider a NS two-terminal normal metal-superconductor Andreev interferometer containing a loop in the N part of the device. Then,

electrons with charge $-e$ from N are Andreev-reflected as holes with charge e and a Cooper with charge $-2e$ is transmitted into S . Doubling the charge for the quartet mechanism, a pair of electron-like quasiparticles with charge $-2e$ can be reflected as a pair of hole-like quasiparticles with charge $2e$ while two Coopers with charge $-4e$ are transmitted into S_c . We investigate in paper III whether this can produce an inversion in the critical current on the quartet line between $\Phi/\Phi_0 = 0$ and $\Phi/\Phi_0 = 1/2$ (for instance in connection with figure 3c in Ref. 24). In addition, we obtain emergence of a small energy scale which is compatible with the experimental observation⁴ of a small voltage scale V_* in the variations of the critical current with voltage V .

The items (A), (B) and (C) above summarize the main motivations of papers I, II and III of the series. Now, we come specifically to the following paper I.

III. THE HAMILTONIANS

This section contains the assumptions about the model. The features of the Harvard group experiment⁴ which are essential to the model are listed in subsection III A. The Hamiltonians are presented next, first the BCS Hamiltonian of the superconducting leads (see subsection III B), next the Hamiltonian of a 2D metal used for the sheet of graphene (see subsection III C), and finally the tunneling Hamiltonian describing the contacts between the 2D metal and the superconducting leads (see subsection III D). The voltage biasing conditions are given in subsection III E. The critical current on the quartet line is defined in subsection III F, in connection with making the link between our calculations and the experiments.

A. The essential ingredients

We start by presenting which ingredients of the Harvard group experiment⁴ are important in our theoretical description.

The model relies on the following facts:

(i) The superconductors are connected on a 2D metal (see the yellow region in figure 1) which consists of graphene gated away from the Dirac point.

(ii) The experiment involves four terminals instead of three in the previous theoretical⁵⁻¹² and experimental^{13,14} papers.

In most of the following work, the discussion is at the level of two limiting cases for the device parameters:

(a) The $V = 0^+$ adiabatic limit is implemented, still with biasing on the quartet line.

(b) The limit of low-transparency interfaces between the 2D metal and the superconducting leads is implemented.

In addition, section IX generalizes the theory to arbitrary values of the interface transparency and bias voltage.

B. BCS Hamiltonian of the superconducting leads

Now, we present the standard BCS Hamiltonian of each superconducting lead taken individually. In zero flux $\Phi/\Phi_0 = 0$, all superconducting leads are described by

$$\mathcal{H}_{BCS} = -W \sum_{\langle i,j \rangle} \sum_{\sigma=\uparrow,\downarrow} \left(c_{i,\sigma}^+ c_{j,\sigma} + c_{j,\sigma}^+ c_{i,\sigma} \right) \quad (7)$$

$$- \Delta \sum_i \left(e^{i\varphi} c_{i,\uparrow}^+ c_{i,\downarrow}^+ + e^{-i\varphi} c_{i,\downarrow} c_{i,\uparrow} \right), \quad (8)$$

where the summation \sum_i is over all tight-binding sites on a cubic lattice, the summation $\sum_{\langle i,j \rangle}$ runs over all pairs of nearest neighbors, and $\sigma = \uparrow, \downarrow$ is the spin. The first term in Eq. (7) is the kinetic energy. The second term given by Eq. (8) is the BCS mean field pairing term with superconducting gap Δ . The macroscopic superconducting phase variable is generically denoted by φ in Eq. (8), and it is assigned the values φ_a , φ_b or φ_c according to which of the superconducting lead S_a , S_b or S_c is considered.

A magnetic field in the loop is taken into account in the following gauge:

$$\varphi_{c,1} = \varphi_c - \frac{\Phi}{2} \quad (9)$$

$$\varphi_{c,2} = \varphi_c + \frac{\Phi}{2}, \quad (10)$$

with a phase gradient along the loop S_c terminated by $S_{c,1}$ and $S_{c,2}$, supposed to have perimeter large compared to the superconducting coherence length.

C. Hamiltonian of the 2D metal

The Hamiltonian of a 2D metal is presented now. The 2D Hamiltonian used to describe the yellow region on figure 1 takes the following form:

$$\mathcal{H}_{2Dmetal} = -W \sum_{\langle i,j \rangle} \sum_{\sigma=\uparrow,\downarrow} \left(c_{i,\sigma}^+ c_{j,\sigma} + c_{j,\sigma}^+ c_{i,\sigma} \right), \quad (11)$$

where the summation $\sum_{\langle i,j \rangle}$ runs over all pairs of neighbors on a square lattice tight-binding lattice in 2D. Eq. (11) is used to model the graphene sheet gated away from the Dirac point in the Harvard group experiment⁴.

D. Tunneling between the superconductors and the 2D metal

Now, we present the tunneling term between the 2D metal and each of the superconducting leads. This coupling Hamiltonian consists of usual hopping between both sides of the junction:

$$\mathcal{H}_{tunnel} = - \sum_{\langle i,j \rangle} \sum_{\sigma=\uparrow,\downarrow} \left(J_{i \rightarrow j} c_{j,\sigma}^+ c_{i,\sigma} + J_{j \rightarrow i} c_{i,\sigma}^+ c_{j,\sigma} \right), \quad (12)$$

where the summation $\sum_{\langle i,j \rangle}$ runs over pairs of the corresponding tight-binding sites on both sides of the contacts. The condition $J_{j \rightarrow i} = (J_{i \rightarrow j})^*$ is a requirement for $\mathcal{H}_{\text{tunnel}}$ to be Hermitian. Plane waves (with conserved component of the wavevector in the direction parallel to the interface) tunnel between each superconducting lead and the 2D metal for a perfectly clean interface *i.e.* if $J_{i \rightarrow j} = J_{j \rightarrow i} \equiv J$ is independent on i, j . But here, we work in the opposite limit of a dirty interface in which tunneling takes place locally as a function of the real-space coordinates along the junctions.

In terms of equations, the amplitude for hopping from i (in the 2D metal layer) to j (the corresponding site in the superconducting lead) is a complex number with a random phase:

$$J_{i \rightarrow j} = J \exp(i\psi_{i \rightarrow j}) \quad (13)$$

$$J_{j \rightarrow i} = J \exp(i\psi_{j \rightarrow i}), \quad (14)$$

where $\psi_{i \rightarrow j} = -\psi_{j \rightarrow i}$ and $\psi_{i \rightarrow j}$ is uniformly distributed in between 0 and 2π . The variables $\psi_{i \rightarrow j}$ and $\psi_{k \rightarrow l}$ are uncorrelated if $i, j \neq k, l$.

This model of a disordered interface was successfully used in previous studies of nonlocal Andreev reflection²⁵ in three-terminal ferromagnet-superconductor-ferromagnet and normal metal-superconductor-normal metal devices.

E. Voltage biasing conditions

The voltage biasing conditions are made explicit in this subsection. The four-terminal ($S_a, S_b, S_{c,1}, S_{c,2}$) device in figure 1 is voltage-biased on the quartet line at (V_a, V_b, V_c, V_c) , with $V_a = -V_b \equiv V$ and $V_c = 0$.

F. A relevant physical quantity

In this subsection, we present the definition of the critical current on the quartet line. This quantity is measured in the Harvard group experiment⁴, and it is evaluated theoretically in the following papers I, II and III. The ‘‘critical current on the quartet line’’ $I_c(V, \Phi/\Phi_0)$ is called in short as ‘‘the critical current’’:

$$I_c(V, \Phi/\Phi_0) = \text{Max}_{\varphi_q} I_S(\varphi_q, V, \Phi/\Phi_0), \quad (15)$$

where $I_c(V, \Phi/\Phi_0)$ is gauge-invariant and the quartet phase φ_q -sensitive $I_S(\varphi_q, V, \Phi/\Phi_0)$ can be calculated in any gauge.

IV. CURRENT-PHASE RELATIONS OF THE QUARTETS AND THE SQ

In this section, we present a simple model for the microscopic processes contributing to the φ_q -sensitive current on the quartet line.

Part of the material presented in sections IV and V is the subject of the Supplemental Material of the Harvard group experimental paper⁴, which is why the presentation is concise in the following two sections.

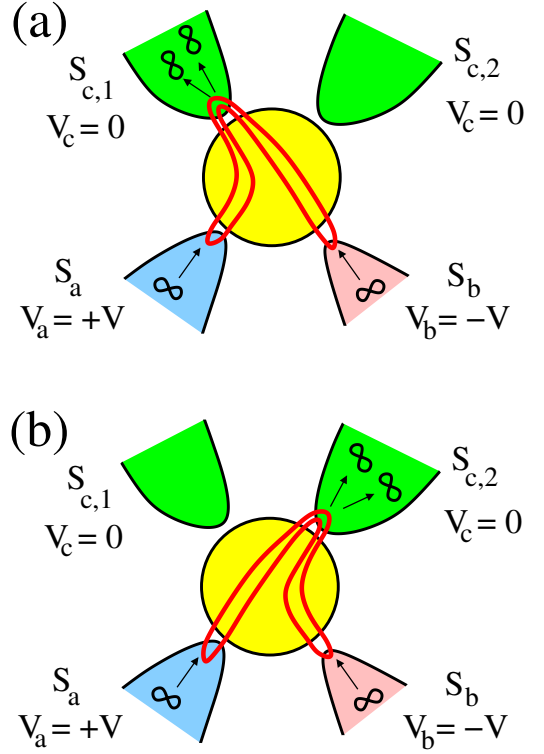


FIG. 3. The lowest-order Q_1 - and Q_2 -quartet diagrams in a real space representation (on panels a and b respectively): Two pairs are taken from (S_a, S_b) biased at $(V, -V)$. After making a quartet from squaring the wave-function of a pair, the two outgoing Cooper pairs are transmitted into the grounded $S_{c,1}$ for the Q_1 -quartets (panel a) or into $S_{c,2}$ for the Q_2 -quartets (panel b). The Q_1 - and the Q_2 -quartet current-phase relations are given by Eqs. (16) and (17) respectively.

Subsection IV A deals with the three-terminal quartets Q_1 and Q_2 transmitted at the $S_{c,1}$ and $S_{c,2}$ contacts. Subsection IV B describes a process of ‘‘statistical fluctuations of the split quartets’’ (FSQ) of order 8 which involves all of the four superconducting leads. Section IV C presents the split quartets (SQ) which are not statistical fluctuations, but produce instead a current proportional to the number of conducting channels.

The Josephson relations given by the following Eqs. (16)-(17) and by Eq. (19) receive the simple interpretation that they are only deduced from counting how many outgoing Cooper pairs are transmitted into $S_{c,1}$ or $S_{c,2}$.

A. The Q_1 and Q_2 -quartets

Now, we consider the three-terminal Q_1 - and Q_2 -quartet diagrams⁵⁻¹² appearing at order-8 in perturbation in the tunneling amplitudes between the 2D metal and the superconducting leads (see figure 3). They transmit four fermions into the same contact, *i.e.* into $S_{c,1}$ for the Q_1 -quartets (see figure 3a) or into $S_{c,2}$ for the Q_2 -quartets (see figure 3b). The

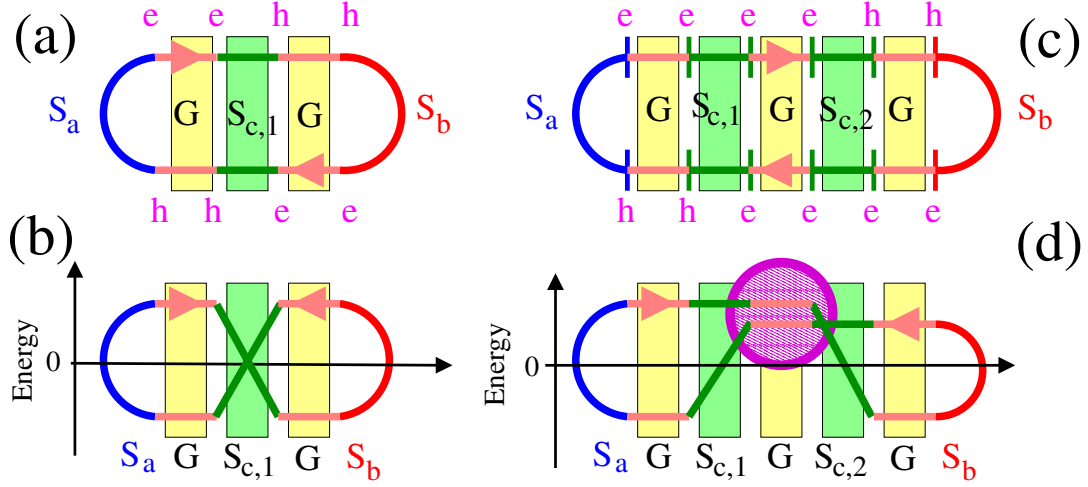


FIG. 4. *Diffuson and energy pictures for the quartets and one of the SQ processes*: Panels a and b represent the Q_1 -quartets in the diffuson and in the energy pictures respectively. Panels c and d show similar representations for the SQ. The sequence of spin-up electron (e) and spin-down hole (h) Nambu labels is indicated on panels a and c. The highlighted region on panel d shows the part of the SQ diagram which corresponds to long range propagation in between $S_{c,1}$ and $S_{c,2}$, which is limited by l_ϕ .

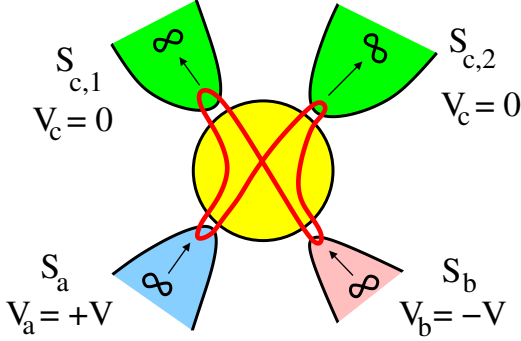


FIG. 5. The diagram encoding *statistical fluctuations of the split quartets (FSQ)* transmits one Cooper pair into $S_{c,1}$ and another one into $S_{c,2}$. The FSQ diagrams encode a statistical fluctuation of the φ_q -sensitive current which does not scale with the number of channels. (This is because the Green's functions cannot be gathered in a pairwise manner on this diagram). The FSQ current-phase relation is given by Eq. (18).

corresponding current-phase relations are the following:

$$I_{Q_1}(\varphi_q, \Phi) = I_{c,Q_1} \sin[\varphi_q + \Phi] \quad (16)$$

$$I_{Q_2}(\varphi_q, \Phi) = I_{c,Q_2} \sin[\varphi_q - \Phi]. \quad (17)$$

The phase variable entering Eq. (16) is $\varphi_a + \varphi_b - 2\varphi_{c,1} \equiv \varphi_q + \Phi$ and that entering Eq. (17) is $\varphi_a + \varphi_b - 2\varphi_{c,2} \equiv \varphi_q - \Phi$, where $\varphi_{c,1}$ and $\varphi_{c,2}$ are given by Eqs. (9) and (10) respectively.

Figures 4a and b show two representations for the Q_1 -quartets:

(i) Figure 4a shows a picture resembling the “diffusons” appearing in the physics of disordered systems.

(ii) Figure 4b shows energy on the y-axis, with respect to the chemical potential of the grounded S_c . This “quartet diagram” was already presented in Ref. 5.

B. The statistical Fluctuations of the Split Quartet current (FSQ)

Before discussing the SQ of order 12 (see the next subsection IV C), we present now a simpler “baby-SQ” of order 8, see figure 5. This order-8 process suffers from producing a current which fluctuates around zero value, both in sign and in amplitude. This is because single-particle Green's functions are necessarily involved in figure 5 if the four contacts make between them distance which is much larger than the Fermi wave-length λ_F . The current associated to this order-8 FSQ process in figure 5 is the following:

$$I_{FSQ}(\varphi_q) = I_{c,FSQ} \sin \varphi_q. \quad (18)$$

The phase variable entering Eq. (18) is given by $\varphi_a + \varphi_b - \varphi_{c,1} - \varphi_{c,2} \equiv \varphi_q$.

C. The “split quartet diagram” (SQ)

Now, we present in this subsection the diagram which realizes quartet splitting.

The lowest-order SQ diagram of order 12 (see figure 6) encodes a total of $2^5 = 32$ different realizations of the electron/hole Nambu labels. A subset of those yields the same $\sim \sin(\varphi_q)$ current as the previous FSQ diagram in figure 5 [see Eq. (18)], without being a statistical fluctuation as it was the case for the FSQ presented above:

$$I_{SQ}(\varphi_q) = I_{c,SQ} \sin(\varphi_q). \quad (19)$$

The diffuson and the energy representations on figure 4c, d respectively illustrate that Eq. (19) is related to two electron-hole conversions taking place at the $S_{c,1}$ and $S_{c,2}$ contacts, instead of two electron-hole conversions at the same $S_{c,1}$ contact for the Q_1 -quartets in figure 4a, b.

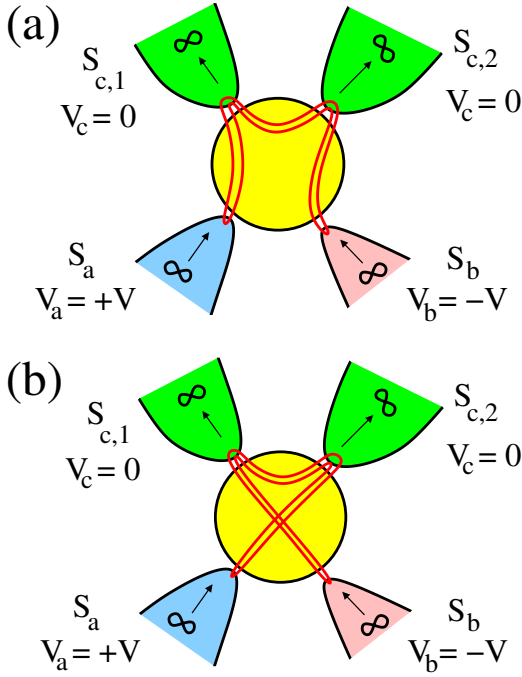


FIG. 6. *The Split Quartet diagrams (SQ) on panels a and b contribute to the current-phase relation given by Eq. (19). The SQ current is nonvanishingly small only if the yellow intermediate region is a 2D metal, as opposed to 1D or 3D metal. Contrary to the previous FSQ diagram (see figure 5), these SQ diagrams yield a φ_q -sensitive current which is not a small statistical fluctuation. On the contrary, the SQ current scales with the number of channels because the corresponding Green's functions are gathered in a pair-wise manner on this figure.*

Section I of the Supplemental Material²⁶ presents a further analysis of the SQ diagram, in connection with how it can be evaluated numerically.

V. INTERFERENCE BETWEEN THE QUARTETS AND THE SQ

We proceed by further considering that the φ_q -sensitive critical current is the result of an interference between the Q_1 - and the Q_2 -quartets (see section IV A) and the SQ (see section IV C):

$$I_c(\Phi/\Phi_0) = \text{Max}_{\varphi_q} [I_{Q_1}(\varphi_q, \Phi) + I_{Q_2}(\varphi_q, \Phi) + I_{SQ}(\varphi_q)] \quad (20)$$

Eq. (20) is now 2π -periodic in Φ , while the previous $\text{Max}_{\varphi_q} [I_{Q_1}(\varphi_q, \Phi) + I_{Q_2}(\varphi_q, \Phi)]$ was π -periodic.

More specifically, specializing to $\Phi/\Phi_0 = 0$ and to $\Phi/\Phi_0 = 1/2$ leads to

$$I_c(0) = |I_{c,Q_1} + I_{c,Q_2} + I_{c,SQ}|, \quad (21)$$

which is different from

$$I_c(1/2) = |I_{c,Q_1} + I_{c,Q_2} - I_{c,SQ}|. \quad (22)$$

VI. WHY THE SQ APPEAR ONLY IN 2D

Now that we have settled the quartet and SQ processes, we proceed with presenting results which are not included in the Supplemental Material of the Harvard group experimental paper⁴. The goal of this section is to discuss why the SQ are specific to a 2D metal in the yellow intermediate region of figure 1, *i.e.* why the SQ yields a vanishingly small current if a 1D or 3D metal is used instead of the 2D metal.

The Green's function calculations are complemented in section VI B by a connection with a general argument about the solutions of the wave equation in D space dimensions. A summary is presented in subsection VI C.

A. Green's function of a 2D metal

In this subsection, we present the necessary Green's function calculation which supports the SQ in 2D.

The asymptotics of Bessel functions yields the following long-distance $k_F R \gg 1$ approximation to the 2D Green's function [see Eqs. (54) and (55) in the Appendix]:

$$g^{A,11}(R) = g^{A,22}(R) \simeq \frac{i}{W\sqrt{k_F R}} \cos\left(kR - \frac{\pi}{4}\right) \quad (23)$$

$$g^{R,11}(R) = g^{R,22}(R) \simeq -\frac{i}{W\sqrt{k_F R}} \cos\left(kR - \frac{\pi}{4}\right). \quad (24)$$

A sanity check of Eqs. (23) and (24) is provided in section II of the Supplemental Material²⁶, for a double junction between a 2D metal and two 3D normal leads.

B. The quantum nanowake effect

Now, we show that this 2D effect can be understood within the more general framework of the wave equation in D space dimensions. Namely, we establish a link between the preceding calculations of section VI A and the general theory of the “wake” appearing in the solutions of the even-dimensional wave equation (see section VI B 1). A wake in nanoscale electronic devices is considered in section VI B 2. Synchronization of Josephson junctions is discussed in section VI B 3, in connection with the SQ diagram shown in figure 4d.

We also make here reference to a very recent preprint²⁷ about the production of quantum wakes with ultracold atoms.

1. The wake effect in the classical wave equation

Volterra was the first to understand that the solution of the wave-equation is drastically different in even or in odd space dimension. Let us assume that an excitation is produced, in a way which is localized in space and in time. A detector is at separation R away from the location of the excitation. In all cases, the signal reaches R after time $t_0 = R/v$, where v is the speed of wave propagation. In odd dimensions (such as in

1D or 3D), the detected signal consists of a sharp pulse corresponding to the wave-front. But in even dimension (such as in 2D), the detected signal oscillates long after time t_0 . This “wake”, which is there in even space dimensions but not in odd dimension, meets everyone’s experience of a boat propagating on a calm sea, or throwing stones into a lake.

2. The quantum nanowake effect in meso- or nanoscale devices

The signal at the detector mentioned above results from a convolution of the initial excitation by the D -dimensional Green’s functions. It turns out that electronic Green’s functions are at the heart of the calculation of transport properties in meso- or nanoscale devices. It is also known that the normal-state Green’s function at distance R is itself a plane-wave in 1D:

$$g_{1D}(R, \omega) \sim \exp(ikR), \quad (25)$$

where k is the wave-vector at the considered energy ω . In 3D, it is also given by the plane-wave

$$g_{3D}(R, \omega) \sim \frac{\exp(ikR)}{kR}, \quad (26)$$

which is normalized by the factor kR arising from probability conservation. In 2D, the Green’s function is a Bessel function which behaves like

$$g_{2D}(R, \omega) \sim i \frac{\cos(kR - \pi/4)}{\sqrt{kR}} \quad (27)$$

at large $R \gg 1/k$ [see Eq. (23) above].

3. Synchronizing two Josephson junctions by the nanowake effect

The difference between the 1D or 3D $\exp(ikR)$ oscillations in Eqs. (25) and (26), and the 2D $\cos(kR - \pi/4)$ oscillations in Eq. (27) is now discussed in connection with synchronizing two Josephson junctions.

Specifically, we focus on the highlighted region of the SQ diagram shown in figure 4d. We determine the robustness of the square of the Green’s function $[g(R)]^2$ in the presence of a multichannel interface simply by averaging $[g(R)]^2$ over R around the value R_0 such that $\lambda_F \ll R_0 \lesssim l_\phi$, where R takes values in an interval of width $\Delta R \sim 2\pi/k$:

$$\langle\langle [g_{1D}(R)]^2 \rangle\rangle = 0 \quad (28)$$

$$\langle\langle [g_{2D}(R)]^2 \rangle\rangle \simeq -\frac{1}{2W^2 k_F R} \quad (29)$$

$$\langle\langle [g_{3D}(R)]^2 \rangle\rangle = 0. \quad (30)$$

As mentioned above, the quantity $\langle\langle [g(R)]^2 \rangle\rangle$ is relevant to the part of the SQ diagram connecting $S_{c,1}$ and $S_{c,2}$, which exchanges a fermion between the $S_{c,1}$ and $S_{c,2}$ contacts (see the highlighted region in figure 4).

Eqs. (28), (29) and (30) are deduced from Eqs. (25), (23) and (26) respectively. These Eqs. (28)-(30) imply long-range coupling over l_ϕ between the contact points $S_{c,1}$ and $S_{c,2}$ if a 2D metal is used, and short range coupling over λ_F if a 1D or a 3D metal is used, which is in agreement with the general theory of the wake in arbitrary dimension.

Thus, it is only in 2D that the diagrams in figures 4c and d are nonvanishingly small, due to $\langle\langle [g(R)]^2 \rangle\rangle$ connecting $S_{c,1}$ and $S_{c,2}$ (see the highlighted region in figure 4d).

C. Summary of this section

The microscopic theory of the SQ was sketched in this section:

(i) The SQ is specific to 2D, and it is related to the properties of the wave-equation in even dimension.

(ii) The SQ realize *quantum mechanical* synchronization between Josephson junctions by coherently exchanging a quasiparticle between them.

(iii) The SQ operate already in the simple limit of equilibrium (with bias voltage $V = 0$), and in the adiabatic limit (with $V = 0^+$ on the quartet line).

We note that the SQ do not contribute to the current in the previous Grenoble group experiment¹³. In this experiment, the intermediate region connecting the superconducting leads consists of an evaporated “T-shaped” Copper lead which is 3D, as opposed to the atomically thin 2D sheet of graphene used in the Harvard group experiment⁴. A quantum nanowake effect is neither expected to play a role in the Weizmann Institute group experiment¹⁴ made with a semiconducting nanowire.

VII. π -SHIFTS OF THE QUARTETS AND THE SQ

Now that we have established the model, we consider the experimental consequences of the overlapping wave-functions for the two Cooper pairs coming from S_a and S_b biased at $\pm V$, which are coupled by the Pauli exclusion principle. We discuss specifically the signs of the quartet current-phase relation (section VII A), of the SQ (see section VII B) and we provide the corresponding numerical calculation in section VII C.

A. π -shift of the quartet current

We start with recalling an intuitive argument for the π -shift of the quartet current-phase relation⁶. The wave-function

$$\frac{1}{\sqrt{2}} \left(c_{a,\uparrow}^+ c_{b,\downarrow}^+ - c_{a,\downarrow}^+ c_{b,\uparrow}^+ \right), \quad (31)$$

of a Cooper pair is squared according to

$$\frac{1}{2} \left(c_{a,\uparrow}^+ c_{b,\downarrow}^+ - c_{a,\downarrow}^+ c_{b,\uparrow}^+ \right)^2, \quad (32)$$

and it is identical to the opposite of a pair of pair:

$$-\left(c_{a,\uparrow}^+c_{a,\downarrow}^+\right)\left(c_{b,\uparrow}^+c_{b,\downarrow}^+\right). \quad (33)$$

The “minus” sign in Eq. (33) is a macroscopic manifestation of the internal structure of a pair, *i.e.* its orbital and spin symmetries.

B. π -shift of the SQ current

We consider now interchanging two fermions in the SQ channel. This yields a “minus” sign originating from the Pauli antisymmetrization principle.

A Cooper pair is transmitted from S_a to $S_{c,1}$ and a second one from S_b to $S_{c,2}$, yielding the following intermediate state:

$$c_{S_{c,1},\uparrow}^+c_{S_{c,1},\downarrow}^+c_{S_{c,2},\uparrow}^+c_{S_{c,2},\downarrow}^+ \quad (34)$$

Exchanging the $(\uparrow, S_{c,1})$ and the $(\uparrow, S_{c,2})$ partners according to the SQ diagram (see figure 4d) leads to a “minus” sign and to a π -shift in the relation between the SQ current and the quartet phase.

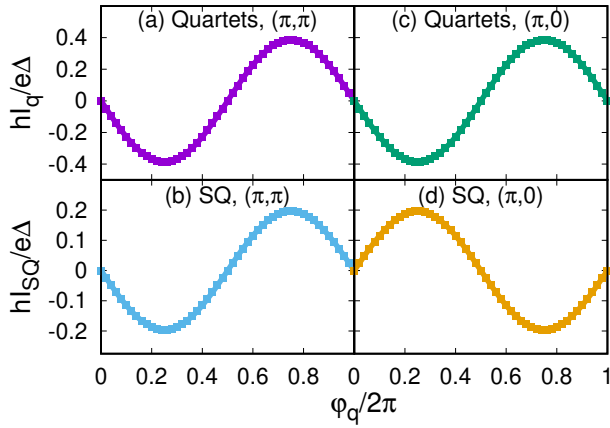


FIG. 7. The zero-flux $\Phi = 0$ quartet and SQ current-phase relations on panels a and b respectively, as they are given by Eq. (16) for the quartets, and by Eq. (19) for the SQ. Panels a and b are obtained from numerical implementation of the lowest-order diagrams in figures 3 and 6. Panels a and b correspond to a (π, π) shift of the quartet and SQ channels, as it is obtained from perturbation theory. Panels c and d show an “artificial” $(\pi, 0)$ junction with π - and 0-shifts: panel c for the quartets is identical to panel a and panel d for the SQ is the opposite of panel b.

C. Comparison with numerical calculations

Now, we evaluate numerically the quartet and SQ currents from lowest order perturbation theory.

The lowest-order three-terminal quartet current $I_q(\varphi_q)$ and the four-terminal SQ current $I_{SQ}(\varphi_q)$ are shown in Fig. 7a and Fig. 7b respectively, as a function of the quartet phase φ_q . The

numerical data are obtained from a microscopic Green’s function calculation based on the tunnel and the adiabatic limit simultaneously taken.

Figure 7a confirms the π -shift in the quartet current as a function of φ_q , see section VII A. Figure 7b confirms the predicted π -shift in the SQ current-phase relation, see section VII B.

We coin figure 7a and b as being “ (π, π) -shifted with respect to the quartet and the SQ channels”, thus with a relative shift of 0 between them.

It is only in the section IV B of the Supplemental Material²⁶ that we comment on figures 7c and d.

VIII. ABSENCE OF INVERSION BETWEEN $\Phi/\Phi_0 = 0$ AND $\Phi/\Phi_0 = 1/2$

In this section, we show that the (π, π) shifts for the quartets and the SQ obtained above in section VII imply noninverted behavior $I_c(0) > I_c(1/2)$ in the reduced flux Φ/Φ_0 dependence of the critical current I_c . In addition, we address the reverse question of the information which can be deduced from “noninverted behavior” regarding the sign of the quartet or SQ current-phase relations. The general assumptions about the 0 and π shifts are presented in section VIII A. The corresponding reasoning is presented in section VIII B. The consequences for the Harvard group experiment are provided in section VIII C. An analogy with a SQUID is presented in section VIII D.

A. The assumptions

This section is based on the following general assumptions:

(i) We have information about the Φ/Φ_0 -sensitivity of the critical current I_c , more specifically about whether $I_c(0)$ is smaller or larger than $I_c(1/2)$.

(ii) The signs of the quartet and the SQ critical currents $I_{c,Q_1} + I_{c,Q_2}$ and $I_{c,SQ}$ are left a free parameters.

B. General statements

In this subsection, we establish a link between the 0- and π -shifts of the quartets and the SQ, and the presence/absence of inversion between $I_c(0)$ and $I_c(1/2)$.

Let us assume specifically that absence of inversion $I_c(0) > I_c(1/2)$ is observed in an experiment. Combining Eqs. (21), (22) to Eq. (10) in section III of the Supplemental Material²⁶ yields the following “logical chain”:

$$I_c(0) > I_c(1/2) \quad (35)$$

$$\iff |I_{c,Q_1} + I_{c,Q_2} + I_{c,SQ}| > |I_{c,Q_1} + I_{c,Q_2} - I_{c,SQ}| \quad (36)$$

$$\iff I_{c,Q_1} + I_{c,Q_2} \text{ and } I_{c,SQ} \text{ have the same sign.} \quad (37)$$

C. Conclusion on the Harvard group experiment⁴

In this subsection, we present consequences for the Harvard group experiment⁴.

Lowest-order perturbation theory in the tunnel amplitudes combined to the adiabatic limit implies “ π -shifted current-phase relations in the quartet and the SQ channels” (see section VII), *i.e.* what we called above as (π, π) shifts in the quartet and SQ channels.

Given that Eq. (37) implies Eq. (35), we conclude that lowest-order perturbation theory implies “Absence of inversion in the critical current $I_c(\Phi/\Phi_0)$ between $\Phi/\Phi_0 = 0$ and $\Phi/\Phi_0 = 1/2$ ”, *i.e.* $I_c(0) > I_c(1/2)$.

Conversely, “Experimental evidence for absence of inversion” does not necessarily imply “ π -shift in both the quartet and the SQ channels taken individually”, because the possibility of 0-shifted quartet and SQ channels is also compatible with “Evidence for absence of inversion”.

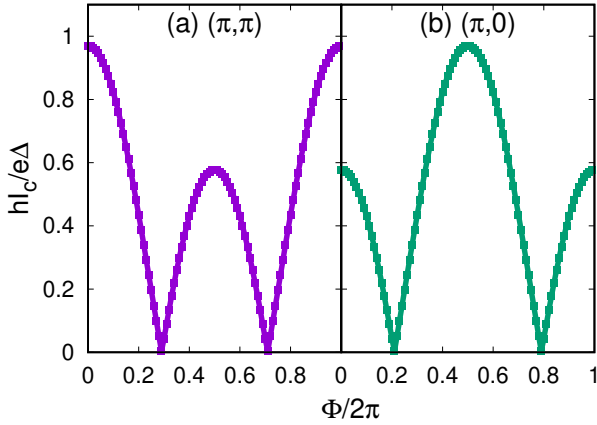


FIG. 8. Flux- Φ dependence of the critical current I_c , for the same (π, π) and $(\pi, 0)$ quartet and SQ channels as on figure 7. We obtain $I_c(0) > I_c(1/2)$ for the (π, π) -shifted quartets and SQ, and the reverse for the $(\pi, 0)$ shifts. We obtain half-period shift of the interference between the (π, π) and the $(\pi, 0)$ shifts in the quartet and SQ channels. This figure confirms the analytical arguments of sections VIII A, VIII B and VIII C.

D. Analogy with interferometric detection of the π -shift²⁸

The Φ/Φ_0 -dependence of the critical current $I_c(\Phi/\Phi_0)$ is shown in figure 8. In addition to the discussion provided in section IV of the Supplemental Material, we provide here the following conclusion on an analogy between the 0 or π -shifts of the quartets and the SQ and a SQUID containing a 0 and a π -junction. This “internal SQUID” analogy is in between:

(i) The half-period shift of the critical current of the SQUID, when changing the pair of (0,0)-shifted Josephson junction into the pair of $(\pi, 0)$ -shifted junctions, see Ref.28.

(ii) The half-period shift in the critical current I_c of the four-terminal Josephson junction shown in figure 8, when changing the (π, π) -shifts of the quartets and SQ into $(\pi, 0)$ -shifts.

IX. GENERALIZATION TO ARBITRARY INTERFACE TRANSPARENCIES AND VOLTAGE

Now, we note that the quartets transmit even number of Cooper pairs into $S_{c,1}$ or $S_{c,2}$ and that the SQ transmit odd number of Cooper pairs. This characterization based on the parity is now generalized to arbitrary values of the interface transparencies and voltage. The following arguments are not based on approximations. On the contrary, they are based on exact results which hold for arbitrary values of the interface transparencies and bias voltage.

We start with the $V = 0^+$ adiabatic limit combined to arbitrary interface transparencies in section IX A. Next, we generalize to arbitrary contact transparency and voltage in section IX B. Finally, we consider in section IX C the consequences for the interpretation of the Harvard group experiment⁴.

A. Generalized Ambegaokar-Baratoff formula

In this subsection, we establish a link between $I_c(0) \neq I_c(1/2)$ and interference between quantum processes transmitting even or odd numbers of Cooper pairs into $S_{c,1}$ or $S_{c,2}$. We start with the $V = 0^+$ adiabatic limit and include arbitrary contact transparencies.

The critical current can be expanded as the following:

$$I'_c(\Phi/\Phi_0) = \text{Max}_{\varphi_c} \sum_{n,p} X(2n, p) \times \sin \left[(2n-p) \left(\varphi_c - \frac{\Phi}{2} \right) + p \left(\varphi_c + \frac{\Phi}{2} \right) \right], \quad (38)$$

where the gauge is given by Eqs. (9) and (10). The variable $X(2n, p)$ in Eq. (38) is a real number. The total number of Cooper pairs is denoted by $2n$: n pairs are taken from the superconducting lead S_a biased at $V_a = +V$, and n others from S_b biased at $V_b = -V$. The integer p in Eq. (38) is the number of Cooper pairs transmitted into the grounded loop S_c at the $S_{c,2}$ contact. Thus, the remaining $2n - p$ pairs are transmitted into the loop S_c at the other $S_{c,1}$ contact.

In the $V = 0^+$ adiabatic limit (but with arbitrary interface transparencies), Eq. (38) has the same status as the Fourier transform of the supercurrent deduced from the Ambegaokar-Baratoff formula for a single weak link connecting two grounded superconductors.

Now, we make the change of variables $\varphi_c \rightarrow \varphi_c + \Phi/2$, which is equivalent to changing the gauge from Eqs. (9)-(10) to $\varphi_{c,1} = \varphi_c$ and $\varphi_{c,2} = \varphi_c + \Phi$:

$$I'_c(\Phi/\Phi_0) = \text{Max}_{\varphi_c} \sum_{n,p} X(2n, p) \sin [(2n-p) \varphi_c + p(\varphi_c + \Phi)]. \quad (39)$$

This Eq. (39) simplifies as

$$I'_c(\Phi/\Phi_0) = \text{Max}_{\varphi_c} \sum_{n,p} X(2n, p) \sin [2n\varphi_c + p\Phi]. \quad (40)$$

It deduced that

$$I'_c(0) = \text{Max}_{\varphi_c} \sum_{n,p} X(2n,p) \sin[2n\varphi_c] \quad (41)$$

$$I'_c(1/2) = \text{Max}_{\varphi_c} \sum_{n,p} X(2n,p)(-)^p \sin[2n\varphi_c]. \quad (42)$$

Separating the terms with p even or odd according to

$$Y_{\text{even}}(\varphi_c) = \sum_{p \text{ even}} \sum_n X(2n,p) \sin[2n\varphi_c] \quad (43)$$

$$Y_{\text{odd}}(\varphi_c) = \sum_{p \text{ odd}} \sum_n X(2n,p) \sin[2n\varphi_c] \quad (44)$$

leads to

$$I'_c(0) = \text{Max}_{\varphi_c} [Y_{\text{even}}(\varphi_c) + Y_{\text{odd}}(\varphi_c)] \quad (45)$$

$$I'_c(1/2) = \text{Max}_{\varphi_c} [Y_{\text{even}}(\varphi_c) - Y_{\text{odd}}(\varphi_c)]. \quad (46)$$

The following logical link is deduced:

“*Experimental observation for different values of the critical current between reduced fluxes $\Phi/\Phi_0 = 0$ and $\Phi/\Phi_0 = 1/2$ at arbitrary transparency*” [i.e. $I'_c(0) \neq I'_c(1/2)$ in Eqs. (45) and (46)]

is equivalent to

“*Evidence for interference between processes transmitting even or odd number of Cooper pairs into $S_{c,1}$ and $S_{c,2}$* ”.

B. Generalization to finite bias voltage on the quartet line

Section V of the Supplemental Material²⁶ demonstrates the intuitive form of the generalized Ambegaokar-Baratoff formula given by Eq. (38) for arbitrary interface transparencies and voltage biasing on the quartet line.

C. Conclusion on the Harvard group experiment⁴

It deduced from the previous section IX B that “Experimental evidence for $I'_c(0) \neq I'_c(1/2)$ ” implies “Evidence for transmission of odd number of Cooper pairs into $S_{c,1}$ or $S_{c,2}$ ”. Since the modes have to be gathered in a pair-wise manner, this implies that each of the superconducting lead $S_{c,1}$ and $S_{c,2}$ contains at least one mode of the SQ type. Our article is concluded with the following:

“*Experimental evidence for different values of the critical currents at $\Phi/\Phi_0 = 0$ and $\Phi/\Phi_0 = 1/2$* ”, i.e. $I'_c(0) \neq I'_c(1/2)$ implies

“*Evidence for the SQ*”.

X. CONCLUSIONS

Now, we proceed with the concluding section. Concluding remarks are presented in section X A and a specific conclusion on the Harvard group experiment⁴ is presented in section X B.

A. Conclusion

Now, we provide a summary of the paper and final remarks.

In this paper, we have provided a general theory of the inversion in the critical current $I_c(\Phi/\Phi_0)$ on the quartet line for a four-terminal Josephson junction (see figure 1), in connection with the recent Harvard group experiment⁴.

Specifically, we based the description on a simple model of Josephson relations deduced from lowest-order perturbation theory in the tunneling amplitudes.

The Harvard group experiment⁴ uses graphene gated away from the Dirac point, which we modeled as a 2D metal with a circular Fermi surface, ignoring the Dirac cones. The SQ do not contribute to the current if a 1D or a 3D metal is used in the yellow region of figure 1 instead of the considered 2D metal. The importance of 2D is related to the general properties of the solutions of the wave equation, which imply a wake in even dimension (such as 2D), but not in odd dimension (such as 1D or 3D). We have demonstrated that a “quantum nanowake” can synchronize two Josephson junctions by the exchange of a quasiparticle at the $S_{c,1}$ and $S_{c,2}$ contacts, yielding a nonvanishingly small synchronized current in the 2D SQ channel.

We have demonstrated that lowest-order perturbation theory produces a π -shift in the quartet and the SQ channels, which implies non-inverted behavior $I_c(0) > I_c(1/2)$. In turn, experimental evidence for noninverted behavior implies the possibilities of either (0,0) or (π,π) shifts for the quartets and the SQ.

We proposed an analogy with a SQUID containing a π - and a 0-shifted Josephson junction²⁸, which is confirmed by our numerical calculations of the reduced flux- Φ/Φ_0 dependence of the critical current $I_c(\Phi/\Phi_0)$. The 0- or π -shifted quartet and SQ channels play the role of the 0- or π -shifted Josephson junctions in the SQUID.

An important conclusion is on the connection between “ $I_{q,c}(0) \neq I_{q,c}(1/2)$ ” and “evidence for the SQ”, whatever the values of the interface transparencies and bias voltage.

Regarding the range of the SQ, it is shown in section VI of the Supplemental Material²⁶ that the SQ are robust against taking the (very) long junction limit $L_x \lesssim l_\varphi$ of the device along the x -axis direction, where l_φ is the mesoscopic phase coherence length of the 2D metal. We conclude that the SQ are a nonstandard “mesoscopic” channel of quantum coherent synchronization, which operates in between the quartets at the smallest scale and the early 1980s synchronization of macroscopic Josephson circuits^{29,30}. An interesting complementary point of view is to approach this mesoscopic regime from the the classical limit, i.e. to incorporate quantum fluctuation in the classical circuit models.

B. Final remarks on the Harvard group experiment⁴

We conclude with what our theory teaches on the Harvard group experimental data⁴.

The first conclusion was already mentioned above, namely, “Experimental evidence for $I_c(0) \neq I_c(1/2)$ ” implies “Evi-

dence for the SQ". Thus, the Harvard group experiment is evidence for the SQ.

The second conclusion is that the part of the experimental data showing $I_c(0) > I_c(1/2)$ is compatible with low-transparency interfaces and with the $V = 0^+$ adiabatic limit (see sections VII and VIII). This conclusion calls for further theoretical developments, in connection with physically motivated approximations for finite values of the voltage and interface transparencies.

ACKNOWLEDGEMENTS

The author acknowledges the stimulating collaboration with the Harvard group (K. Huang, Y. Ronen and P. Kim) to sections IV A and IV B. The author wishes to thank R. Danneau and B. Douçot for their collaboration on an early attempt to find signatures of the quantum nanowake in the signal of multiple Andreev reflection through bilayer graphene. R. Danneau also provided useful comments on an early version of the manuscript. The author acknowledges fruitful discussions with D. Feinberg. The author thanks the Infrastructure de Calcul Intensif et de Données (GRICAD) for use of the resources of the Mésocentre de Calcul Intensif de l'Université Grenoble-Alpes (CIMENT).

GREEN'S FUNCTION OF A 2D METAL

We start this Appendix with the following Fourier transform for the Green's function connecting two tight-binding sites separated by distance R :

$$g^{A,11/22}(R, \omega) = \int_{-\pi}^{\pi} d\theta \int_0^{+\infty} \frac{kdk}{(2\pi)^2} \exp(ikR \cos \theta) g^{A,11/22}(\mathbf{k}, \omega), \quad (47)$$

where

$$g^{A,11}(\mathbf{k}, \omega) = \frac{1}{\omega - \xi_{\mathbf{k}} - i\eta} \quad (48)$$

$$g^{A,22}(\mathbf{k}, \omega) = \frac{1}{\omega + \xi_{\mathbf{k}} - i\eta}, \quad (49)$$

with $\xi_{\mathbf{k}}$ the kinetic energy of the 2D plane-wave state \mathbf{k} with respect to the chemical potential $\mu = \hbar^2 k_F^2 / 2m$, where k_F and m are the Fermi wave-vector and the band-mass respectively. The superscript "11" or "22" in Eqs. (47)-(49) refer to propagation in the electron-electron or hole-hole channels respectively.

Eq. (47) can be rewritten as

$$g^A(R, \omega) = \int_0^{+\infty} \frac{kdk}{(2\pi)} \frac{J_0(kR)}{\omega - \varepsilon \xi_{\mathbf{k}} - i\eta}, \quad (50)$$

where the Bessel function

$$J_0(x) = \frac{1}{2\pi} \int_{-\pi}^{\pi} \exp(ix \cos \theta) d\theta \quad (51)$$

was introduced in Eq. (50). The parameter ε takes the values $\varepsilon = \pm 1$ for the 11 and 22 components. We consider a pole at

$$k \equiv k_0 \simeq k_F + \frac{\varepsilon(\omega - i\eta)}{v_F}, \quad (52)$$

with v_F the Fermi velocity. The residue is evaluated according to

$$\omega - \varepsilon \xi_{k_0 + \delta k} - i\eta \simeq -\frac{\hbar^2}{2m} \varepsilon k_0 \delta k \simeq -\varepsilon v_F k_0 \delta k. \quad (53)$$

Considering in addition that $\text{sign}(\text{Im}k_0) = -\varepsilon$ and using contour integration in the complex k plane leads to

$$g^{A,11}(R) = g^{A,22}(R) = \frac{i}{W} J_0(k_F R) \quad (54)$$

$$g^{R,11}(R) = g^{R,22}(R) = -\frac{i}{W} J_0(k_F R). \quad (55)$$

The long-distance behavior of Eqs. (54) and (55) is given by Eqs. (23) and (24).

-
- ¹ P. W. Anderson, *Random-Phase Approximation in the Theory of Superconductivity*, Phys. Rev. **112**, 1900 (1958).
 - ² P. W. Anderson, *Plasmons, Gauge Invariance, and Mass*, Phys. Rev. **130**, 439 (1963).
 - ³ B.D. Josephson, *Possible new effects in superconductive tunnelling*, Physics Letters **1**, 251 (1962).
 - ⁴ K.F. Huang, Y. Ronen, R. Mélin, D. Feinberg, K. Watanabe, T. Taniguchi and P. Kim, *Quartet supercurrent in a multi-terminal Graphene-based Josephson Junction*, cond-mat preprint (2020).
 - ⁵ A. Freyn, B. Douçot, D. Feinberg and R. Mélin, *Production of non-local quartets and phase-sensitive entanglement in a superconducting beam splitter*, Phys. Rev. Lett. **106**, 257005 (2011).
 - ⁶ T. Jonckheere, J. Rech, T. Martin, B. Douçot, D. Feinberg, and R. Mélin, *Multipair DC Josephson resonances in a biased allsuper-*

- conducting bijunction*, Phys. Rev. B **87**, 214501 (2013).
- ⁷ J. Rech, T. Jonckheere, T. Martin, B. Douçot, D. Feinberg, and R. Mélin, *Proposal for the observation of nonlocal multipair production*, Phys. Rev. B **90**, 075419 (2014).
- ⁸ R. Mélin, D. Feinberg and B. Douçot, *Partially resummed perturbation theory for multiple Andreev reflections in a short three-terminal Josephson junction*, Eur. Phys. J. B **89**, 67 (2016).
- ⁹ R. Mélin, M. Sotito, D. Feinberg, J.-G. Caputo and B. Douçot, *Gate-tunable zero-frequency current cross-correlations of the quartet mode in a voltage-biased three-terminal Josephson junction*, Phys. Rev. B **93**, 115436 (2016).
- ¹⁰ R. Mélin, J.-G. Caputo, K. Yang and B. Douçot, *Simple Floquet-Wannier-Stark-Andreev viewpoint and emergence of low-energy scales in a voltage-biased three-terminal Josephson junction*,

- Phys. Rev. B **95**, 085415 (2017).
- ¹¹ R. Mélin, R. Danneau, K. Yang, J.-G. Caputo, and B. Douçot, *Engineering the Floquet spectrum of superconducting multiterminal quantum dots*, Phys. Rev. B **100**, 035450 (2019).
 - ¹² B. Douçot, R. Danneau, K. Yang, J.-G. Caputo and R. Mélin, *Berry phase in superconducting multiterminal quantum dots*, Phys. Rev. B **101**, 035411 (2020).
 - ¹³ A. H. Pfeffer, J. E. Duvauchelle, H. Courtois, R. Mélin, D. Feinberg, and F. Lefloch, *Subgap structure in the conductance of a three-terminal Josephson junction*, Phys. Rev. B **90**, 075401 (2014).
 - ¹⁴ Y. Cohen, Y. Ronen, J.H. Kang, M. Heiblum, D. Feinberg, R. Mélin and H. Strikman, *Non-local supercurrent of quartets in a three-terminal Josephson junction*, Proc. Natl. Acad. Sci. U. S. A. **115**, 6991 (2018).
 - ¹⁵ J. E. Zimmerman and A. H. Silver, *Macroscopic Quantum Interference Effects through Superconducting Point Contacts*, Phys. Rev. **141**, 367 (1966).
 - ¹⁶ J.D. Pillet, V. Benzoni, J. Griesmar, J.-L. Smir and Ç. Ö. Girit, *Nonlocal Josephson Effect in Andreev Molecules* Nano Lett. **19**, 7138 (2019).
 - ¹⁷ J.-D. Pillet, V. Benzoni, J. Griesmar, J.-L. Smir and Ç. Ö. Girit, *Scattering description of Andreev molecules*, SciPost Phys. Core **2**, 009 (2020).
 - ¹⁸ R.-P. Riwar, M. Houzet, J.S. Meyer, and Y.V. Nazarov, *Multi-terminal Josephson junctions as topological materials*, Nat. Commun. **7**, 11167 (2016).
 - ¹⁹ E. Eriksson, R.-P. Riwar, M. Houzet, J. S. Meyer, and Y. V. Nazarov, *Topological transconductance quantization in a four-terminal Josephson junction*, Phys. Rev. B **95**, 075417 (2017).
 - ²⁰ E. Strambini, S. D'Ambrosio, F. Vischi, F.S. Bergeret, Yu.V. Nazarov, and F. Giazotto, *The ω -SQUIPT as a tool to phase-engineer Josephson topological materials*, Nat. Nanotechnol. **11**, 1055 (2016).
 - ²¹ A.W. Draelos, M.-T. Wei, A. Seredinski, H. Li, Y. Mehta, K. Watanabe, T. Taniguchi, I.V. Borzenets, F. Amet, and G. Finkelstein, *Supercurrent flow in multiterminal graphene Josephson junctions*, Nano Lett. **19**, 1039 (2019).
 - ²² N. Pankratova, H. Lee, R. Kuzmin, M. Vavilov, K. Wickramasinghe, W. Mayer, J. Yuan, J. Shabani, and V.E. Manucharyan, *The multi-terminal Josephson effect*, arXiv:1812.06017 (2019).
 - ²³ G. Falci, D. Feinberg F.W.J. Hekking, *Correlated tunneling into a superconductor in a multiprobe hybrid structure*, Europhys. Lett. **54**, 255 (2001).
 - ²⁴ T. H. Stoof and Yu. V. Nazarov, *Flux effect in superconducting hybrid Aharonov-Bohm rings*, Phys. Rev. B **54**, R772(R) (1996).
 - ²⁵ R. Mélin and D. Feinberg, *Sign of the crossed conductances at a ferromagnet/superconductor/ferromagnet double interface*, Phys. Rev. B **70**, 174509 (2004).
 - ²⁶ See the Supplemental Material which contains technical details of the calculations.
 - ²⁷ M. Wampler, P. Schauss, E. B. Kolomeisky, and I. Klich, *Quantum wakes in lattice fermions*, arXiv: 2006.09466v1 (2020).
 - ²⁸ W. Guichard, M. Aprili, O. Bourgeois, T. Kontos, J. Lesueur, and P. Gandit, *Phase Sensitive Experiments in Ferromagnetic-Based Josephson Junctions*, Phys. Rev. Lett. **90**, 167001 (2003).
 - ²⁹ M. A. H. Nerenberg, J. A. Blackburn, and D. W. Jillie, *Voltage locking and other interactions in coupled superconducting weak links. I. Theory*, Phys. Rev. B **21**, 118 (1980).
 - ³⁰ D. W. Jillie, M. A. H. Nerenberg, and J. A. Blackburn, *Voltage locking and other interactions in coupled superconducting weak links. II. Experiment*, Phys. Rev. B **21**, 125 (1980).